Jpn. J. Appl. Phys. Vol. 39 (2000) pp. L 1283–L 1285
Part 2, No. 12B, 15 December 2000

Dark Current in Quantum Dot Infrared Photodetectors

Victor RYZHII, Victor PIPA[1], Irina KHMYROVA, Vladimir MITIN[1] and Magnus WILLANDER[2]

Computer Solid State Physics Laboratory, University of Aizu, Aizu-Wakamatsu 965-8580, Japan
[1]*Department of Electrical and Computer Engineering, Wayne State University, Detroit 48202, U.S.A.*
[2]*Department of Microelectronics and Nanoscience, Chalmers University of Technology and Gothenburg University, Gothenburg S-412 96, Sweden*

(Received September 19, 2000; accepted for publication November 6, 2000)

We present the results of a new analytical model for the analysis of the dark current in realistic quantum dot infrared photodetectors (QDIPs). This model includes the effect of the space charge formed by electrons captured in QDs and donors, the self-consistent electric potential in the QDIP active region, the activation character of the electron capture and its limitation by the Pauli principle, the thermionic electron emission from QDs and thermionic injection of electrons from the emitter contact into the QDIP active region, and the existence of the punctures between QDs. The developed model yields the dark current as a function of the QDIP structural parameters, applied voltage, and temperature. It explains some features of the dark current characteristics observed experimentally.

KEYWORDS: quantum dot, infrared photodetector, donor, space charge, dark current

Heterostructure diodes with a quantum dot layer inserted between heavily doped contacts can serve as infrared photodetectors utilizing bound-to-continuum transitions. Such quantum dot infrared photodetectors (QDIPs) were proposed and analyzed theoretically by one of the authors[1)] (see, also ref. 2). Recently,[3–12)] several research groups reported the fabrication and extensive experimental study of various InAs/GaAs, InGaAs/GaAs, and InGaAs/InGaP QDIPs. Although expected to have advantages over quantum well infrared photodetectors (QWIPs) with similar parameters, most of the investigated QDIPs exhibited characteristics inferior to those of QWIPs (see, for example, refs. 13 and 14). The prediction of high performance for QDIPs was based on the device model[1,2)] that assumes dense QD layers with a nearly uniform lateral distribution of the electric potential. In such an ideal QDIP, small but lightly coupled QDs preserve their sensitivity to normally incident infrared radiation[15)] and their low capture probability due to the effect of phonon bottleneck[16)] maintaining a more or less uniform in-plane distribution of the captured electrons. In contrast, the QDIPs investigated in the recent experiments contained relatively large QDs placed far apart. As a result, even substantially charged QD layers did not form planar potential barriers which could effectively control the electron transport. It was shown[17)] that the presence of the potential repulsive barriers surrounding the charged QDs substantially decreases the probability of electron capture. Thus, the analysis of such realistic QDIPs under dark current conditions and under illumination, requires a more complex model than the existing ones.

In this paper we develop an analytical model for the dark current in realistic QDIPs. We describe the QDIP dark current characteristics, taking into account the following: the influence of the space charge of electrons captured in QDs and the space charge created by donors on the spatial distribution of the electric potential in the QDIP active region; the activation character of the electron capture and its limitation by the Pauli principle; the thermionic electron emission from QDs and thermionic injection of electrons from the emitter contact into the QDIP active region; and the existence of the punctures between QDs through which a significant portion of the injected electrons flows.

The QDIP under consideration consists of a QD structure which includes a series of QD (InAs or InGaAs) layers separated by a wide-gap material (GaAs, InGaP, and so on). Each QD layer comprises uniformly distributed identical QDs with the density Σ_{QD} which have a disk-like shape. The QD layers can be doped by donors whose density is equal to Σ_D. It is assumed that the lateral characteristic size of QDs a_{QD} (the QD lateral area is equal to a_{QD}^2) is sufficiently large, so that each of them has a large number of bound states and, consequently, is capable of accepting relatively large numbers of electrons. Conversely, the transverse size of QDs, l_{QD}, is assumed to be relatively small, providing the existence of a single energy level associated with the quantization in this direction. It is also small in comparison with the spacing between the QD layers L (transverse period of the QDIP structure). The QD structure is clad between doped contact regions made of the same material as the barrier region between QD layers. These regions play a role of the QDIP emitter and collector. A schematic view of the QDIP structure is shown in Fig. 1.

The current arising under applied voltage is determined by the potential distribution in the QDIP active region. This distribution depends, in turn, on the space charge formed by electrons occupying QDs and donors. The space charge of mobile electrons is, as in QWIPs, usually very small and can be neglected. In QDIPs with large QDs which can capture a large average number of electrons, one can assume that the

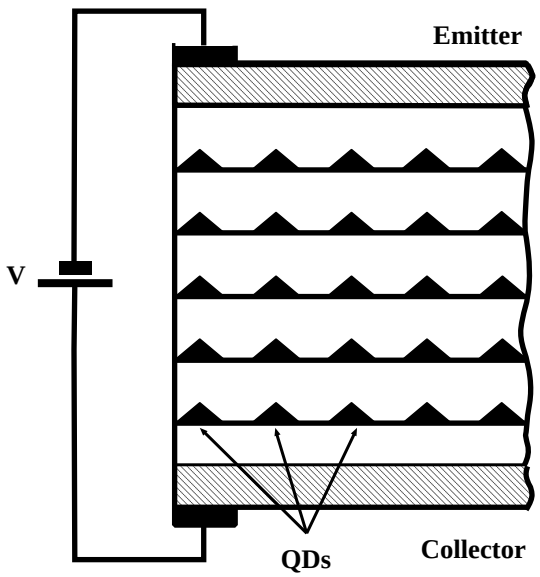

Fig. 1. Schematic view of the QDIP structure.

charges of QDs belonging to the same QD layer are approximately equal. Thus, the average number of electrons in a QD belonging to the kth QD layer $\langle N_k \rangle$ can be indicated by a solitary QD layer index k ($k = 1, 2, \ldots K$, where K is the total number of the QD layers in the QDIP). The numbers of electrons captured into the QDs with index k is governed by an equation describing the balance of electrons captured into QDs and excited from them. In dark conditions, assuming that the main mechanism of the electron escape from QDs is associated with their thermoemission and that the transport of electrons across the QDIP active region is due to their drift, the balance equation can be presented as:

$$\langle j \rangle p_k = e \Sigma_{QD} G_k, \tag{1}$$

where $\langle j \rangle$ is the current density averaged in the in-plane directions, $e = |e|$ is the electron charge, G_k is the rate of the electron thermoexcitation from QDs and p_k is the capture probability. The latter two quantities are governed by the following equations, respectively:

$$G_k = G_0 \exp\left(-\frac{\varepsilon_{QD}}{k_{BT}}\right) \exp\left(\frac{\pi \hbar^2 \langle N_k \rangle}{m k_{BT} a_{QD}^2}\right), \tag{2}$$

$$p_k = p_0 \frac{N_{QD} - \langle N_k \rangle}{N_{QD}} \exp\left(-\frac{e^2 \langle N_k \rangle}{C k_B T}\right). \tag{3}$$

In eqs. (2) and (3), G_0 is the pre-exponential factor, ε_{QD} is the ionization energy of the ground state in QDs, m is the effective mass of electrons in QDs and $\hbar$ and k_B are the Planck and Boltzmann constants, respectively. T is the temperature, p_0 is the capture parameter for uncharged QWs, N_{QD} is the maximum number of electrons which can occupy each QD, $C \simeq (2æ a_{QD}/\pi\sqrt{\pi})$ is the QD capacitance, and æ is the dielectric constant. Equations (1)–(3) are akin to those for QWIPs.[18–21]

Considering the range of not too low voltages, $eV > eV_0 \gg k_{BT}$, where $eV_0 \simeq \varepsilon_{QD}$ is the height of the potential barrier in the QDIP active region at equilibrium, the local dark current density can be presented in the following form:

$$j = j_m \exp\left[\frac{e(\langle \varphi_1 \rangle + \Delta\varphi_1)}{k_B T}\right], \tag{4}$$

where j_m is the maximum current density which can be extracted from the emitter contact. Equation (4) assumes that because $eV > eV_0 \gg k_{BT}$, the ridge of the potential barrier limiting the electron injection from the emitter contact, is in the first QD layer plane. In eq. (4), the electric potential of the QD layer with $k = 1$ is presented as the sum of the average potential formed by all QDs and donors $\langle \varphi_1 \rangle$ at the plane $z = L$ and the potential $\Delta\varphi_1 = \Delta\varphi_1(x, y)$ created at this plane by the QDs nearest to a given puncture in the potential barrier. Here, coordinate z corresponds to the direction perpendicular to the QD layer plane (growth direction), while x and y are the in-plane coordinates. The average potential is governed by the Poisson equation in which the space charge is averaged in the in-plane directions. Noting that according to eqs. (1)–(3) numbers $\langle N_k \rangle$ are actually the same for all indexes (i.e., $\langle N_k \rangle = \langle N \rangle$), the Poisson equation for the average potential can be reduced to the following:

$$\frac{d^2 \langle \varphi \rangle}{d z^2} = \frac{4\pi e}{æ} \sum_{k=1}^{K} (\langle N \rangle \Sigma_{QD} - \Sigma_D)\, \delta(z - kL). \tag{5}$$

Solving eq. (5) with boundary conditions $\langle \varphi \rangle|_{z=0} = 0$ and $\langle \varphi \rangle|_{z=(N+1)L} = V$, where V is the applied bias voltage, we obtain

$$\langle \varphi_1 \rangle = \frac{V}{(K+1)} - \frac{2\pi K e L}{æ} (\langle N \rangle \Sigma_{QD} - \Sigma_D). \tag{6}$$

It is natural to assume that the propagation of electrons through a puncture between QDs is affected, apart from by the average potential, by the potential created by the four QDs surrounding this puncture, thus (for example, for the puncture with lateral coordinates $x = y = 0$), one can arrive at

$$\Delta\varphi_1 = \frac{4\sqrt{2}\langle N \rangle \sqrt{\Sigma_{QD}}}{æ} \left[\xi - \frac{1}{2}\Sigma_{QD}(x^2 + y^2)\right], \tag{7}$$

where $\xi = \sqrt{2}\ln[(1+\sqrt{5})(2+\sqrt{5})/2]/\sqrt{2} - 1 \simeq 0.361$. Using eqs. (4), (6), and (7), for the average current density

$$\langle j \rangle = \Sigma_{QD} \int_{-L_{QD}/2}^{L_{QD}/2} \int_{-L_{QD}/2}^{L_{QD}/2} j\, dx dy,$$

after integration we obtain

$$\langle j \rangle \simeq j_m \left(\frac{2\Theta}{\langle N \rangle}\right) \times \exp\left[e\left(V + V_D - \frac{\langle N \rangle}{N_{QD}} V_{QD}\right) \Big/ (K+1) k_B T\right]. \tag{8}$$

Here, we have introduced parameters

$$\Theta = \frac{æ k_B T}{4\sqrt{2} e^2 \sqrt{\Sigma_{QD}}},$$

$$V_{QD} = \frac{2\pi e}{æ} K(K+1)\Sigma_{QD} L (1 - \eta) N_{QD},$$

and

$$V_D = \frac{2\pi e}{æ} K(K+1)\Sigma_D L,$$

where $\eta = (2\sqrt{2}\xi/\pi K L \sqrt{\Sigma_{QD}})$.

Using eq. (1) with eqs. (2) and (3), we obtain

$$\langle N \rangle \left(1 + \frac{\sqrt{\pi} a_{QD}}{2 a_B}\right) = N_0 + \frac{m k_B T a_{QD}^2}{\pi \hbar^2} \ln\left[\frac{\langle j \rangle p_0 (N_{QD} - \langle N \rangle)}{e G_0 \Sigma_{QD} N_{QD}}\right], \tag{9}$$

where $a_B = æ\hbar^2/me^2$ is the Bohr radius and $N_0 = (m a_{QD}^2 \varepsilon_{QD}/\pi\hbar^2) \simeq N_{QD}$.

Coupled eqs. (8) and (9) govern $\langle j \rangle$ and $\langle N \rangle$ as functions of the QDIP structural parameters, applied bias voltage, and temperature.

At moderate voltages $V_0 < V \ll (V_{QD} - V_D)$, when $\langle N \rangle$ is markedly smaller than N_{QD}, one can neglect the dependence of the logarithmic term in eq. (9) on $\langle N \rangle$. In contrast, at relatively high voltages $V \leq (V_{QD} - V_D)$, this dependence is important, and eq. (9) yields $\langle N \rangle \simeq N_{QD}$. In these two limiting cases, using eqs. (8) and (9), we obtain the following equations for $\langle j \rangle$:

$$\langle j \rangle \simeq j_0\, \theta^{1/\gamma} \exp\left[\left(\frac{e(V + V_D)}{(K+1)} - (\gamma - 1)\varepsilon_{QD}\right) \Big/ \gamma k_B T\right], \tag{10}$$

for $V_0 < V \ll (V_{QD} - V_D)$, and

$$\langle j \rangle \simeq j_0\,\theta\,\exp\left[\frac{e(V+V_{\rm D}-V_{\rm QD})}{(K+1)k_{\rm B}T}\right]. \qquad (11)$$

for $V \le (V_{\rm QD}-V_{\rm D})$. Here,

$$j_0 = \frac{eG_0\Sigma_{\rm QD}}{p_0},$$

$$\theta = \left(\frac{j_m}{j_0}\right)\left(\frac{2\Theta}{N_{\rm QD}}\right)$$

and

$$\gamma = 1 + 2K\Sigma_{\rm QD}a_{\rm QD}^2\left(\frac{L}{a_{\rm B}}\right)\left[\frac{1-\eta}{1+(\sqrt{\pi}a_{\rm QD}/2a_{\rm B})}\right].$$

As can be seen from eqs. (10) and (11), the dark current exhibits an exponential increase with increasing applied bias voltage as well as with increasing doping level. Figure 2 shows the calculated and experimental[9] dark current-voltage characteristics of InAs/GaAs QDIPs. In the calculations, we assumed that $K = 10$, $\Sigma_{\rm QD} = (1.2-1.6)\times 10^{10}\,{\rm cm}^{-2}$, $L = 100\,{\rm nm}$, $a_{\rm QD} = 15\,{\rm nm}$, and $a_{\rm B} = 15\,{\rm nm}$ at $T = 40\,{\rm K}$. Comparison of the theoretical and experimental results reveals their good agreement. Thus, the developed model, which takes into account the features of electron transport in QDIPs and, primarily, the features of the space charge formation, provides an explanation for the elevated steepness of the QDIP dark current–voltage characteristics observed experimentally.[7,9] In some cases,[22] QDIPs exhibited yet more steep dark current–voltage characteristics than those in ref. 9 and given by eq. (10). The analysis shows that the dark current–voltage characteristics of QDIPs with fairly high doping levels (with about five donors per dot) obtained experimentally[22] are in a reasonable agreement with eq. (11). In such QDIPs, the characteristic voltage $V_{\rm QD}-V_{\rm D}$ is moderate, thus, except for a narrow range of applied voltages, inequality $V \ll V_{\rm QD}-V_{\rm D}$ is not valid, and QDs are totally filled.

It is worth noting that the dark current-temperature dependence given by eq. (10) corresponds to an effective activation energy which can be markedly smaller than the ground state ionization energy $\varepsilon_{\rm QD}$. Indeed, eq. (10) yields $\varepsilon_A \simeq (1-\gamma^{-1})\varepsilon_{\rm QD}$. The value of γ obtained in the above calculations and in the experiment[9] is 2.6. Consequently, $\varepsilon_A/\varepsilon_{\rm QD} \simeq 0.6$. A similar effect of decreased activation energy was observed in QWIPs with thermionic injection[23] whose operation is very similar to that of QDIPs. Equation (10) also elucidates why the dark current in real QDIPs is fairly high, exeeding that in QWIPs with comparable parameters. The point is that usually the parameter of the QDIP "nonideality" $\Sigma_{\rm QD}a_{\rm QD}^2$ is rather small that leads to γ close to unity and a low activation energy. As a rough approximation, the QWIP dark-current characteristics can be obtained from the above formulas by setting $\Sigma_{\rm QD}a_{\rm QD}^2 = 1$ and $\eta = 0$ in the expression for parameter γ resulting in a higher value of this parameter for QWIPs than that for QDIPs. Thus, an increase in the product, $\Sigma_{\rm QD}a_{\rm QD}^2$, should favor lower dark current in QDIPs. Because the dark current and, predictably, the photocurrent rise strongly with increasing doping of the QDIP active region, the doping level is an important parameter for the optimization of QDIPs.

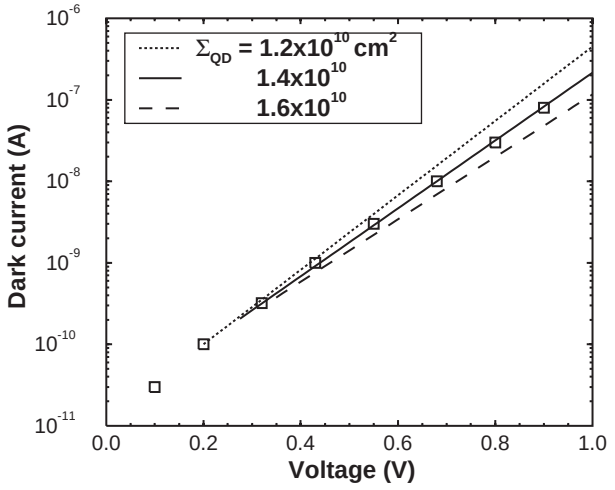

Fig. 2. Comparison of calculated (lines) and experimental (squares) dark current–voltage characteristics.

In summary, we developed an analytical model for realistic QDIPs and used this model for the calculation of the dark current as a function of the structural parameters, applied bias voltage and temperature. Our results clarify experimental observations of sharp dark current–voltage characteristics of QDIPs as well as strong dependence of the dark current on the density of QDs in the QD layers and the doping level of the active region. The calculated characteristics of QDIPs are in good agreement with those obtained experimentally.

Acknowledgment

The authors are thankful to Professor H. Sagawa for useful information and to N. Tsutsui for technical assistance. The work at WSU was supported by the U.S. Army Research Office.

1) V. Ryzhii: Semicond. Sci. Technol. **11** (1996) 759.
2) V. Ryzhii, M. Ershov, I. Khmyrova, M. Ryzhii and T. Iizuka: Physica B **227** (1996) 17.
3) J. Phillips, K. Kamath and P. Bhattacharya: Appl. Phys. Lett. **72** (1998) 2020.
4) S. Kim, H. Mohseni, M. Erdtmann, M. Michel, J. Jelen and M. Razeghi: Appl. Phys. Lett. **73** (1998) 963.
5) D. Pan, E. Towe and S. Kennerly: Appl. Phys. Lett. **73** (1998) 1937.
6) S. Maimon, E. Finkman, G. Bahir, S. E. Schacham, J. M. Garcia and P. M. Petroff: Appl. Phys. Lett. **73** (1998) 2003.
7) S. J. Xu, S. J. Chua, T. Mei, X. C. Wang, X. H. Zhang, H. G. Karunasiri, W. J. Fan, C. H. Wang, J. Jiang, S. Wang and X. G. Xie: Appl. Phys. Lett. **73** (1998) 3153.
8) N. Horiguchi, T. Futatsugi, Y. Nakata, N. Yokoyama, T. Mankad and P. M. Petroff: Jpn. J. Appl. Phys. **38** (1999) 2559.
9) J. Phillips, P. Bhattacharya, S. W. Kennerly, D. W. Beekman and M. Dutta: IEEE J. Quantum Electron. **35** (1999) 936.
10) D. Pan, E. Towe and S. Kennerly: Appl. Phys. Lett. **75** (1999) 2719.
11) L. Chu, A. Zrenner, G. Böhm and G. Abstreiter: Appl. Phys. Lett. **75** (1999) 3599.
12) S.-W. Lee, K. Hirakawa and Y. Shimada: Appl. Phys. Lett. **75** (1999) 1428.
13) B. F. Levine: J. Appl. Phys. **74** (1994) R1.
14) A. Rogalski: Infrared Phys. Technol. **38** (1997) 295.
15) M. Helm: in *Intersubband Transitions in Quantum Wells: Physics & Device Application*, eds. H. C. Liu and F. Capasso (Academic Press, San Diego, 2000) p. 1.
16) U. Bockelmann and G. Bastard: Phys. Rev. B **42** (1990) 8947.
17) V. V. Mitin, V. I. Pipa, A. V. Sergeev, M. Dutta and M. Stroscio: in *Abstracts of 24th Workshop on Compound Semiconductor Devices & Integratrd Circuits* (Aegean Sea, Greece, 2000) p. XIY-15.
18) V. Ryzhii and M. Ershov: J. Appl. Phys. **78** (1995) 1214.
19) L. Thibaudeau, P. Bois and J. Y. Duboz: J. Appl. Phys. **79** (1996) 446.
20) V. Ryzhii: J. Appl. Phys. **81** (1997) 6442.
21) V. Ryzhii and H. C. Liu: Jpn. J. Appl. Phys. **38** (1999) 5815.
22) E. Towe and D. Pan: IEEE J. Sel. Topics Quant. Electron. **6** (2000) 408.
23) A. G. U. Perera, S. G. Matsik, H. C. Liu, M. Gao, M. Buchanan, W. J. Schlaff and W. Yeo: Appl. Phys. Lett. **77** (2000) 741.